THE JOURNAL OF PHYSICAL CHEMISTRY B

Article

pubs.acs.org/JPCB

Heterogeneous Crystallization on Pairs of Pre-Structured Seeds

Swetlana Jungblut* and Christoph Dellago

Faculty of Physics, University of Vienna, Boltzmanngasse 5, 1090 Wien, Austria

Supporting Information

ABSTRACT: Studying the effects of small pre-structured seeds on the crystallization transition in an undercooled monodisperse Lennard-Jones fluid with transition interface path sampling combined with molecular dynamics simulations, we analyze the impact of the simultaneous presence of two seeds with various structures. In the presence of seeds with face- and body-centered cubic structures, we find that decreasing the seed-to-seed distance enhances the probability of the crystalline clusters formed on one of the seeds to grow beyond the critical size, thus, increasing the crystal nucleation rates. In contrast, when seeds have an icosahedral structure, the crystalline clusters form mostly in the bulk. The crystal nucleation rate, however, is also determined by the distance between the seeds with regular structure in which the lattice spacing is equal to the bulk lattice constant, pointing to a heterogeneous crystal nucleation that occurs away from the icosahedrally structured seeds. For slightly squeezed seeds, the effects of the presence of seeds with face- and body-centered cubic structures are reduced in comparison to the regular seeds, and we do not see any effect of the presence of the second seed for seeds with squeezed icosahedral structure.

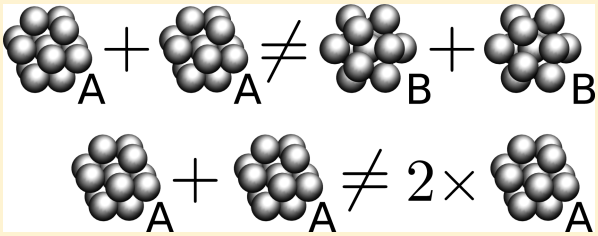

INTRODUCTION

Understanding of the solidification of a liquid is significant for the preparation, design, and processing of crystalline materials.[1] The microscopic details of this transition, however, had been concealed before the development of computer simulations and experimental setups considering colloidal particles permitted a direct visualization of the process.[2−5] This development also facilitated a systematic investigation of the transition kinetics by the intentional manipulation of the boundary conditions. Currently, particular attention is paid to the process of heterogeneous crystallization either in the presence of container walls or small impurities naturally appearing in most physical systems, for example, ice nucleation on atmospheric dust particles.[6]

Recent investigations of the crystallization on a spherical impurity performed in colloidal systems[7] and computer simulations of hard spheres[8] revealed that relatively small impurities with a diameter below a certain value influence the mechanism of the crystal nucleation but not its rate, while larger impurities induce heterogeneous crystal nucleation with a rate higher than the one of a homogeneous process. At the late stages of the transition, however, the spherical impurity which initially acted as a nucleation site may frustrate the growth process of the crystals.[9,10] Further studies analyzed the impacts of planar[11−14] and patterned surfaces[15−26] indicating that, while a flat substrate drastically reduces the free energy barrier to the crystalline phase by favoring the formation of the initial crystalline layer at the wall even at pre-transition conditions, the effect of a rough substrate strongly depends on the commensurability of the wall and crystal structures. Similarly, pre-structured clusters, templates, and impurities of finite size[8,10,27−32] influence the transition to a degree which is determined by the commensurability of the structures, supersaturation, and the size of the additives. In a two-dimensional system, the growth of the crystalline phase in the presence of two seeds had been investigated within density functional theory, revealing that the relative orientation of the seeds is an additional factor that controls the properties of the final phase.[32]

Here, we investigate the cooperative effects of two tiny seeds with various structures and with varying and fixed relative distances on the process of crystal nucleation. Previously, we have found that single seeds with either body-centered cubic (bcc) or face-centered cubic (fcc) structures influence the transition pathways together with the crystal nucleation rates.[33−35] The extent of the effects depends on the structure of the seeds but also on the degree of undercooling. Namely, a regular seed (its lattice constant is equal to the bulk lattice constant) with fcc structure produces a larger increase of the crystal nucleation rate than a regular seed with bcc structure at a moderate undercooling. At a stronger undercooling, this effect is reversed and the largest crystal nucleation rate is obtained in the presence of a regular bcc seed. In the case of a small lattice mismatch between the seed and bulk crystal structures (squeezed seeds) the effects are reduced. In contrast, when the structure of the considered seed is incommensurate to the bulk crystalline structure, in our case icosahedral (icos), the crystal nucleation rate is not significantly affected by the presence of the seeds. The crystals tend to nucleate somewhere in the bulk but not in the vicinity of the seeds (this excluded

Received: June 28, 2016
Revised: July 28, 2016
Published: August 1, 2016

DOI: 10.1021/acs.jpcb.6b06510
J. Phys. Chem. B 2016, 120, 9230−9239

volume is however too small to modify the reaction rate). When the icosahedral seed is slightly squeezed, crystalline clusters sometimes form also on the seed and, as it turns out, reproduce the icosahedral structure of the seed, similarly to the crystals forming on bcc and fcc seeds. As the crystals grow to macroscopic dimensions, these structural effects disappear and the structural composition of crystalline clusters formed by homogeneous crystal nucleation is recovered.

From the classical point of view, seeds with structures (partly) commensurate with the bulk crystalline structure are expected to act as nucleation sites, and the reaction rate should increase proportional to the number of these sites present in the system. On the other hand, we have seen previously that the presence of a regular icosahedral seed suppressed crystal nucleation in the close vicinity of the seed.[34] The volume excluded for nucleation was relatively small, thus, although the volume accessible for homogeneous crystal nucleation was reduced, the reaction rate was not significantly modified. For the current study, we hypothesized that a combination of the increase of the excluded volume due to the presence of two seeds and of the decrease of the total volume of the system might allow us to trace the reduction of the crystal nucleation rate caused by the presence of icosahedral seeds. The actual simulations revealed though that the process of crystal nucleation is more intricate and that the seeds of most of the structures considered here interact in a nontrivial way during the transition process. We find that crystal nucleation rates are determined not only by the number and structure of the seeds but also by the distance between them.

SIMULATION DETAILS

We perform molecular dynamics (MD) simulations of 30 systems of particles interacting via the truncated and shifted Lennard-Jones (LJ) potential with a cutoff distance of $r_c = 2.5$ (in LJ units, which we use throughout the paper). We integrate the equations of motion at the constant pressure and constant enthalpy (*NpH* ensemble[36]) with a time step of $\Delta t = 0.01$ and the pressure set close to zero ($p = 0.003257$). The number of particles and the enthalpy values (collected in Table 1) vary between the systems. The seeds are modeled as a set of particles connected by fixed bonds but are allowed to move translationally and rotationally as a whole.[37] We consider three different types of the seeds. The icosahedral and fcc-structured seeds contain 13 particles, while bcc seeds are made up of 15 particles. In each seed, there is one central particle and the remainder is arranged around it to form the corresponding structure (which includes the first neighbor shell for the fcc and icosahedral seeds, while the bcc seed also contains parts of the second shell). The distance between the central particle and the particles in the first shell is either equal to the distance between the neighbors on a regular lattice, that is, $d = 1.09$, or slightly smaller, $d = 1.0$, resulting in seeds with squeezed structures.

There are two seeds of the same structure in every system considered, and we model the change of seed concentration by varying the number of freely moving particles, adjusting the average volume of the simulation box accordingly. For comparison and in order to ensure that our systems are large enough to assume that finite-size effects are negligible, we also simulate the homogeneous systems of three different sizes.

We prepare the initial configurations in several steps. First, a very large system without seeds is equilibrated and undercooled to the initial state by a periodic rescaling of the velocities of the particles (*NpT* ensemble[36,38]). Then, we cut the obtained configuration into simulation boxes with edge lengths of $L = 18$, 22, and 26 by removing particles outside of these boxes and insert the seeds, simultaneously removing particles for which the interaction energy with one of the seed particles is larger than the largest interparticle interaction energy of the fluid without seeds. The initial positions of the mobile seeds are (0,0,0) and (L/2,0,0). In addition, for the largest box size and two regular ($d = 1.09$) seeds, we fix the distance between the seeds (and their relative orientation) at $D = 9$, 11, and 13, such that the initial positions of the seeds with fixed distance are ($\pm D$/2, 0, 0). Then, we prepare 100 realizations of each system by randomizing the velocities of all particles in a given configuration and again equilibrate (10^5 time steps) the obtained sets at $T = 0.525$ (25% undercooling), computing the average enthalpy per particle. The latter is used to set the initial temperature in the actual simulations of crystal nucleation in the *NpH* ensemble. The enthalpy values together with the respective numbers of particles are collected in Table 1. There, and throughout the paper, we label the seeds with squeezed structures by the subscript 1.0 and regular seeds by the subscript 1.09. We also use the initial edge lengths of the simulation boxes to refer to different system sizes as *L*18, *L*22, and *L*26 and the fixed distances between the seeds to indicate the corresponding systems as *D*9, *D*11, and *D*13.

Table 1. Number of Particles and Enthalpy per Particle

	*L*18	*L*22	*L*26
N, $bcc_{1.0}$	4928	9118	15969
H/N, $bcc_{1.0}$	−6.00267	−5.98958	−5.98286
N, $bcc_{1.09}$	4922	9113	15961
H/N, $bcc_{1.09}$	−6.00022	−5.98786	−5.98224
N, $fcc_{1.0}$	4938	9125	15978
H/N, $fcc_{1.0}$	−5.99879	−5.98741	−5.9818
N, $fcc_{1.09}$	4930	9120	15970
H/N, $fcc_{1.09}$	−5.998	−5.9869	−5.98144
N, $icos_{1.0}$	4938	9127	15978
H/N, $icos_{1.0}$	−5.99569	−5.9855	−5.9807
N, $icos_{1.09}$	4931	9123	15972
H/N, $icos_{1.09}$	−5.99193	−5.98402	−5.9799
N, no seed	4904	8430	16016
H/N, no seed	−5.97391	−5.97363	−5.97361
	*D*9	*D*11	*D*13
N, $bcc_{1.09}$	15957	15962	15961
H/N, $bcc_{1.09}$	−5.98273	−5.98283	−5.98292
N, $fcc_{1.09}$	15968	15973	15968
H/N, $fcc_{1.09}$	−5.98217	−5.9822	−5.98208
N, $icos_{1.09}$	15970	15968	15970
H/N, $icos_{1.09}$	−5.98052	−5.98036	−5.98036

In the main part of our simulations, we employ the transition interface path sampling (TIS) technique to sample trajectories connecting the undercooled liquid state to the crystalline phase.[39−41] In doing so, we use the number of particles in the largest crystalline cluster, n_s, to differentiate between the initial and the final states of the transition, and to define interfaces along the way from the initial to the final states. The crystalline clusters are identified by means of the Steinhardt bond order parameters[42] within the scheme proposed by ten Wolde, Ruiz-Montero, and Frenkel[43] and with optimized crystallinity threshold values.[44]

To increase the sampling efficiency, we set the positions of the TIS interfaces such that the probability to reach the next window is at least 10%. We also make sure that the border of

DOI: 10.1021/acs.jpcb.6b06510
J. Phys. Chem. B 2016, 120, 9230−9239

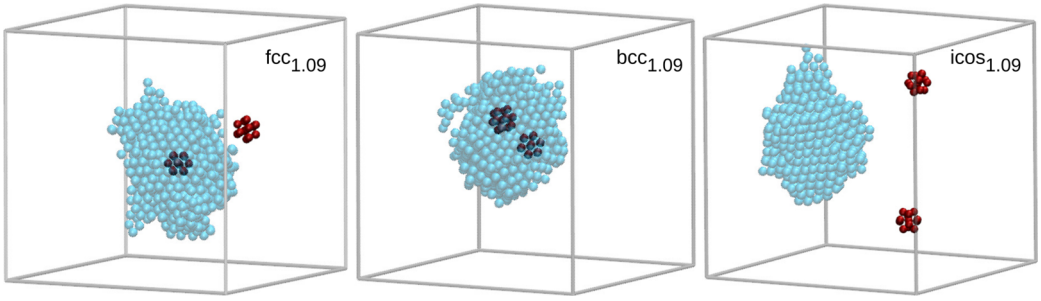

Figure 1. Snapshots of crystalline clusters formed on mobile $fcc_{1.09}$, $bcc_{1.09}$, and $icos_{1.09}$ seeds (from left to right). Particles which do not belong to the largest crystalline cluster are not shown. Seed particles are presented by red spheres. The configurations in which either one or both seeds belong to the largest crystalline clusters (blue spheres) are characteristic for the seeds with cubic structure. Icosahedral seeds are usually not part of the crystalline phase.

the initial state is easily reached on the time scale of a straightforward MD simulation but, at the same time, the system does not leave this state for too long periods of time. Thus, the set of interfaces for systems with fcc-structured seeds is $n_I^{fcc} = \{25, 40, 60, 90, 130, 200\}$ and $n_I^{bcc} = \{25, 40, 60, 90, 130, 180, 240\}$ for systems with bcc-structured seeds. The borders of the initial state are $n_0^{fcc} = n_0^{bcc} = 20$. For homogeneous systems and icosahedrally structured seeds, we place the interfaces at $n_I^{icos} = n_I^{no\ seed} = \{15, 30, 50, 70, 110, 170, 250\}$ and the border of the initial state is $n_0^{icos} = n_0^{no\ seed} = 10$. The number of attempted TIS moves, including 90% of shooting and 10% of path reversal moves, is 10^4 for sampling and at least 10^3 for equilibration. We set the time interval between two shooting points along a trajectory to $\Delta t = 0.1$ and the magnitude of the momentum change for shooting moves such as to obtain an acceptance ratio of 20−40%.

The flux through the first interface is computed from a set of straightforward MD simulations (10^5 time steps). Ensuring that the system under consideration does not crystallize on the time scale of these simulations, we obtain the value of the flux as the number of times the system crosses the first TIS interface coming directly from the border of the initial state per amount of time the system spends below the first TIS interface in one simulation.

Finally, the mechanism of the crystal nucleation is analyzed on the sample of 100 transition paths, which we randomly select out of the set of trajectories that reach the last TIS interface and integrate them to the crystalline cluster size of $n_s \geq 1000$. In Figure 1, we show snapshots of crystalline clusters found in the final configurations of this integration.

RESULTS AND DISCUSSION

Reaction Rates. Within TIS, the reaction rate J, that is, the number of nucleation events per unit time and unit volume, is computed as a product of the flux f_{first}, from the initial state ($n_s \leq n_0$) through the first interface n_{first} and the probability, $P(n_{last}|n_{first})$, to reach the final state of the reaction, given that the system initially started at $n_s \leq n_0$ and crossed the first interface:

$$J = \frac{f_{first}}{V} P(n_{last}|n_{first}) \quad (1)$$

where V is the average volume of the simulation box. Here, we use the last TIS interface to mean the final state of the reaction, which is justified by the fact that the position of this interface is determined by the condition that the probability to continue to the fully crystalline state from there becomes unity.

In Table 2, we summarize the values for the nucleation rates computed for all systems considered. We also include the average values for the flux through the first interface and the volume of the box, computed in a straightforward MD

Table 2. Average Flux f_{first}, Volume, V, and Nucleation Rate, J, for All Systems. Values in Bold Indicate the Largest and the Smallest Nucleation Rates

	f_{first}	V	J
$bcc_{1.0}$			
*L*26	0.164 ± 0.005	17505.9 ± 0.03	(1.8 ± 0.5) × 10^{-10}
*L*22	0.172 ± 0.007	10005.2 ± 0.02	(5.7 ± 1.8) × 10^{-10}
*L*18	0.222 ± 0.016	5417.92 ± 0.02	(5.3 ± 1.4) × 10^{-9}
$bcc_{1.09}$			
*L*26	0.315 ± 0.011	17501.4 ± 0.03	(2.2 ± 0.8) × 10^{-9}
*L*22	0.304 ± 0.008	10004.4 ± 0.02	(4.4 ± 1.6) × 10^{-9}
*L*18	0.361 ± 0.017	5415.73 ± 0.02	(2.4 ± 0.6) × 10^{-8}
*D*13	0.287 ± 0.007	17501.6 ± 0.03	(4.4 ± 1.5) × 10^{-10}
*D*11	0.298 ± 0.007	17502.8 ± 0.03	(7.3 ± 2.3) × 10^{-10}
*D*9	0.302 ± 0.008	17497.5 ± 0.03	(1.9 ± 0.5) × 10^{-9}
$fcc_{1.0}$			
*L*26	0.050 ± 0.003	17512.3 ± 0.03	(1.7 ± 0.5) × 10^{-10}
*L*22	0.051 ± 0.003	10009.6 ± 0.02	(2.5 ± 0.9) × 10^{-10}
*L*18	0.049 ± 0.004	5425.55 ± 0.01	(1.4 ± 0.3) × 10^{-9}
$fcc_{1.09}$			
*L*26	0.205 ± 0.007	17506.5 ± 0.03	(7.2 ± 1.7) × 10^{-9}
*L*22	0.199 ± 0.006	10007.1 ± 0.02	(1.6 ± 0.5) × 10^{-8}
*L*18	0.225 ± 0.007	5419.72 ± 0.02	**(5.7 ± 1.6) × 10^{-8}**
*D*13	0.204 ± 0.006	17504.7 ± 0.03	(3.1 ± 0.8) × 10^{-9}
*D*11	0.209 ± 0.007	17510.0 ± 0.03	(3.7 ± 1.1) × 10^{-9}
*D*9	0.216 ± 0.006	17504.6 ± 0.06	(7.0 ± 2.1) × 10^{-9}
$icos_{1.0}$			
*L*26	0.118 ± 0.002	17514.4 ± 0.03	(1.3 ± 0.4) × 10^{-11}
*L*22	0.071 ± 0.002	10013.8 ± 0.02	(1.1 ± 0.4) × 10^{-11}
*L*18	0.036 ± 0.001	5427.39 ± 0.02	(9.0 ± 3.5) × 10^{-12}
$icos_{1.09}$			
*L*26	0.118 ± 0.002	17511.8 ± 0.03	(2.8 ± 0.9) × 10^{-11}
*L*22	0.066 ± 0.002	10013.6 ± 0.02	(1.7 ± 0.6) × 10^{-11}
*L*18	0.037 ± 0.002	5424.27 ± 0.02	(2.1 ± 0.8) × 10^{-11}
*D*13	0.122 ± 0.003	17510.2 ± 0.03	(3.5 ± 1.0) × 10^{-11}
*D*11	0.114 ± 0.002	17508.0 ± 0.03	(1.0 ± 0.3) × 10^{-11}
*D*9	0.121 ± 0.002	17509.9 ± 0.03	**(6.4 ± 2.5) × 10^{-12}**
no seed			
*L*26	0.118 ± 0.002	17535.4 ± 0.03	(1.4 ± 0.4) × 10^{-11}
*L*22	0.066 ± 0.002	9229.72 ± 0.02	(1.5 ± 0.6) × 10^{-11}
*L*18	0.033 ± 0.001	4931.2 ± 0.02	(1.1 ± 0.3) × 10^{-11}

DOI: 10.1021/acs.jpcb.6b06510
J. Phys. Chem. B 2016, 120, 9230−9239

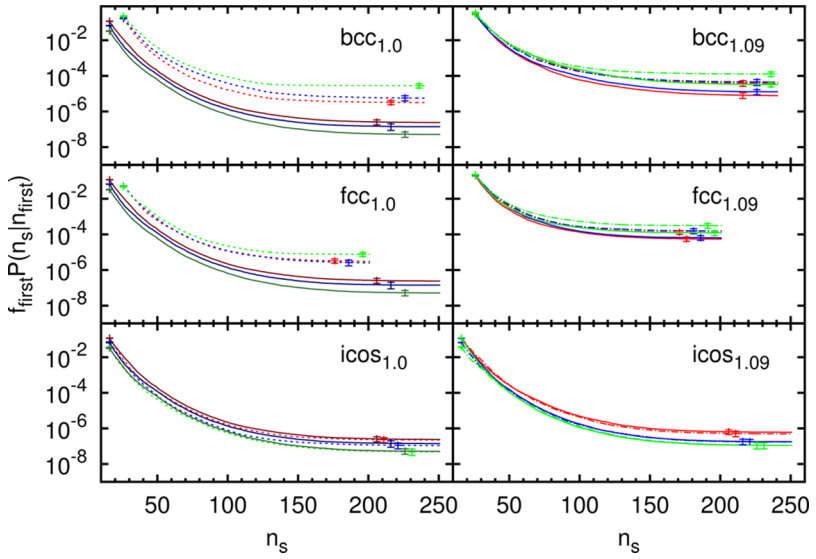

Figure 2. Reactive positive flux, $f_{first}P(n_s|n_{first})$, as a function of the size of the largest crystalline cluster, n_s, converges to a plateau with the value of the corresponding reaction rate constant (the respective rate is then obtained by dividing by the average volume of the initial phase). For mobile squeezed (dashed lines, left column) and regular (dash-dotted lines, right column) seeds, the colors indicate the size of the box, increasing from green (*L*18) through blue (*L*22) to red (*L*26). For seeds with fixed distance (solid lines, right column), colors stand for the distance between the seeds, increasing in the same order from *D*9 (green) to *D*11 (blue) and *D*13 (red). Three homogeneous reference systems of different sizes (roughly corresponding to the boxes with mobile seeds) are indicated by the dark solid lines in the left column, also increasing with the box size from dark green (*L*18) through dark blue (*L*22) to dark red (*L*26). The statistical errors are indicated only for selected points.

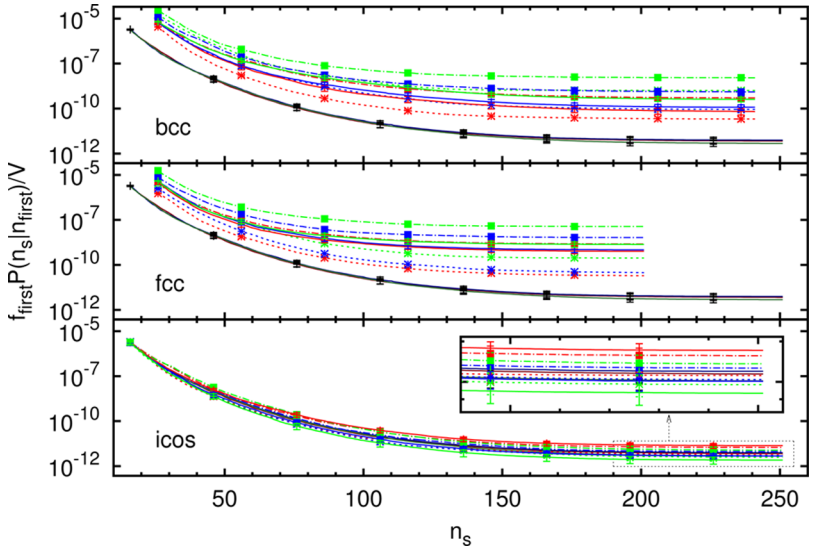

Figure 3. Reactive positive flux density, $f_{first}P(n_s|n_{first})/V$, as a function of the size of the largest crystalline cluster, n_s, in the presence of bcc, fcc, and icosahedral seeds. The inset in the bottom frame magnifies the region indicated by a square on the main plot. For mobile squeezed (dashed lines) and regular (dash-dotted lines) seeds, the colors indicate the size of the box, increasing from green (*L*18) through blue (*L*22) to red (*L*26). For seeds with fixed distance (solid lines), colors stand for the distance between the seeds, increasing in the same order from *D*9 (green) to *D*11 (blue) and *D*13 (red). Three homogeneous reference systems of different sizes (as expected, the data collapses to a single line with the deviation for the smallest box size attributed to the occurrence of minute finite size effects) are indicated by the dark solid lines, also increasing with the box size from dark green (*L*18) through dark blue (*L*22) to dark red (*L*26). The statistical errors are indicated only for selected points.

simulation of the initial state. The evolution of the positive reactive flux $f_{first}P(n_s|n_{first})$ and of the flux density $f_{first}P(n_s|n_{first})/V$ with the increasing cluster size n_s is presented in Figures 2 and 3, respectively. Shortly after the system has crossed the free energy barrier which opposes the nucleation, this flux (density) develops a plateau, the value of which is used to determine the reaction rate.

As can be inferred from Table 2 and Figure 3, reaction rates obtained in the presence of seeds with different structures vary within about 4 orders of magnitude (the largest and the smallest values of the crystal nucleation rate are indicated in Table 2). The rates measured in the presence of icosahedral seeds with different structures are similar to those of a homogeneous system and lie in the lower range of the list. In contrast, the presence of all seeds with cubic structure significantly enhances crystal nucleation and the magnitude of the effect is determined by the specific structure.

DOI: 10.1021/acs.jpcb.6b06510
J. Phys. Chem. B 2016, 120, 9230−9239

In addition to its dependence on the structure, the flux out of the initial state is affected by the size of the simulation box. The way in which it varies with the system size gives a hint at the mechanism of the transition. For example, a constant (initial) flux seen for varying box volume points at heterogeneous crystal nucleation, where, for a constant number of seeds, the probability of the formation of the crystalline cluster on the seeds does not depend on the volume of the system. In contrast, a constant (initial) flux density (*i.e.*, the flux is proportional to the volume) is a feature of homogeneous crystal nucleation. In Table 3, we summarize the data for the initial flux out of the initial state obtained in the presence of one and two seeds of given structure. Overall, we indeed see an occurrence of heterogeneous crystal nucleation in the presence of cubic seeds and of homogeneous crystal nucleation in the presence of icosahedral seeds. A closer look at the values presented in Table 3 reveals, however, that there are also finite size effects due to interactions between cubic seeds and, for single seeds, due to a mixed occurrence of homogeneous and heterogeneous crystal nucleation. The interaction between cubic seeds is reflected in a moderate increase of the reactive flux for the smallest system considered, while the occurrence of homogeneous nucleation in the presence of a single seed can be recognized in the increase of the flux values with the system size.

Table 3. Average Flux f_{first} in the Presence of One and Two Mobile Seeds in Systems of Different Sizes. The Last Column Represents the Ratio of These Fluxes

	$f_{first}^{one\ seed}$	$f_{first}^{two\ seeds}$	#2/#1
$bcc_{1.0}$			
*L*26	0.085 ± 0.003	0.164 ± 0.005	1.93
*L*22	0.082 ± 0.003	0.172 ± 0.007	2.10
*L*18	0.078 ± 0.003	0.222 ± 0.016	2.85
$bcc_{1.09}$			
*L*26	0.163 ± 0.006	0.315 ± 0.011	1.93
*L*22	0.144 ± 0.005	0.304 ± 0.008	2.11
*L*18	0.147 ± 0.005	0.361 ± 0.017	2.46
$fcc_{1.0}$			
*L*26	0.029 ± 0.002	0.050 ± 0.003	1.72
*L*22	0.022 ± 0.002	0.051 ± 0.003	2.32
*L*18	0.023 ± 0.002	0.049 ± 0.004	2.13
$fcc_{1.09}$			
*L*26	0.110 ± 0.005	0.205 ± 0.007	1.86
*L*22	0.095 ± 0.004	0.199 ± 0.006	2.09
*L*18	0.099 ± 0.005	0.225 ± 0.007	2.27
$icos_{1.0}$			
*L*26	0.121 ± 0.003	0.118 ± 0.002	0.98
*L*22	0.064 ± 0.002	0.071 ± 0.002	1.11
*L*18	0.036 ± 0.001	0.036 ± 0.001	1.00
$icos_{1.09}$			
*L*26	0.122 ± 0.002	0.118 ± 0.002	0.97
*L*22	0.068 ± 0.002	0.066 ± 0.002	0.97
*L*18	0.034 ± 0.001	0.037 ± 0.002	1.09

The more pronounced effects caused by the presence of the second seed can be seen in the evolution of the reactive flux along the transition as seen in Figure 2. For regular seeds with fixed seed-to-seed distances and moving cubic seeds, the initially coinciding values of the reactive flux evolve differently with the increasing cluster size. For moving icosahedral seeds, the influence of the second seed is seen on the evolution of the reactive flux density, which at the border of the initial state is independent of the system volume and the structure of the seeds, but deviates from the homogeneous flux density values for larger crystalline clusters. These differences here are rather small and we found that the comparison of the reactive fluxes with those of homogeneous systems in matched volumes is more conclusive on this issue. As demonstrated in Figure 2, the presence of the second squeezed icosahedral seed is not essential for the final value of the reaction rate. In contrast, the evolution of the reactive flux in the presence of regular icosahedral seeds coincides with the reactive fluxes found for fixed seed-to-seed distances.

Evidently, the presence of cubic and icosahedral seeds has quite different effects on the crystallization transition, thus, in the following, we consider them separately.

Face- and Body-Centered Cubic Seeds. The presence of fcc and bcc seeds enhances crystal nucleation, and the magnitude of the effect is determined by the specific structure as well as by the size of the system. As a whole, seeds with regular fcc structure in the smallest volume cause the largest increase and squeezed fcc seeds in the largest volume cause the smallest increase of the crystal nucleation rate. For a given system size, squeezed bcc seeds yield a larger enhancement of the crystallization probability than squeezed fcc seeds, but the effect of regular bcc seeds is smaller than the one of regular fcc seeds. At the same time, the flux out of the initial state in the presence of regular bcc seeds is larger than that in the presence of regular fcc seeds. Furthermore, as can be inferred from Table 3, adding a second seed roughly doubles the initial flux. The exact values, however, tend to slightly increase with the decreasing simulation box size. There are two factors contributing to this effect. First, two seeds present in the smallest system apparently are so close to each other that the presence of the second seed stabilizes the cluster nucleating on the other seed. Second, the initial flux in the presence of a single seed with cubic structure shows a minor increase for the largest simulation box volume considered. Apparently, the presence of a single seed in the smaller systems suppresses homogeneous nucleation in the initial state, which becomes more probable as the volume of the system increases. Certainly, as we discuss next, the evolution of these small clusters nucleating homogeneously to larger dimensions is less probable than of those nucleated heterogeneously. Nevertheless, the presence of a squeezed bcc seed in the largest simulated volume and of a squeezed fcc seed in all systems produced an initial flux density that was smaller than the homogeneous flux density (see Supporting Information). In larger systems, the initial flux density in the presence of two squeezed fcc seeds was smaller than the one found in homogeneous systems. Most likely, these are the effects of partial incommensurability of the seeds with squeezed structure to the bulk crystalline structure, which is also reflected and more pronounced in the tendency of the clusters leaving the initial state to evolve to macroscopic dimensions.

In a previous analysis of crystal nucleation on regular bcc and fcc seeds,[34] we concluded that the transition follows the Ostwald's step rule,[45,46] which states that the evolution of a system proceeds by the route of the smallest free energy difference. That is, a metastable system may transform into its final state through formation of an intermediate phase if the free energy barrier separating the initial from the intermediate state is lower than the one separating the initial from the final thermodynamically most stable state. In LJ crystals, the

DOI: 10.1021/acs.jpcb.6b06510
J. Phys. Chem. B 2016, 120, 9230−9239

intermediate phase corresponds to the bcc structure, while the most stable phase has the fcc structure. Earlier studies of the bulk transformation of an undercooled LJ fluid[41,43,47] confirmed that the crystallization indeed proceeds through the formation of an intermediate bcc phase. From this point of view, the initial reduction of the height of the free energy barrier due to the presence of single seeds with regular bcc and fcc structures is comparable (and even slightly larger for the bcc seed) but then the crystalline clusters with bcc structure formed on the corresponding seed still have to transform into the more stable fcc structure, which is reflected in a decrease of the probability to proceed to larger cluster sizes relative to the respective value in the presence of an fcc seed. Here, we recover a similar picture for a pair of regular seeds. In contrast, the presence of squeezed fcc seeds decreases the height of the free energy barrier less than the presence of squeezed bcc seeds, as can be inferred from the flux values given in Table 2. Hence the final crystal nucleation rate in the presence of squeezed bcc seeds is larger than in the presence of squeezed fcc seeds, although there is a relative drop in the reactive flux along the transition for squeezed bcc seeds. This decrease is best seen in the largest volume, where the final crystal nucleation rates in the presence of squeezed bcc and fcc seeds are comparable. For smaller volumes, we encountered the influence of the second seed, which tends to stabilize the crystalline cluster formed on the other seed when close to it. The last observation also applies to other bcc and fcc seeds. That is, for a given structure, the impact of the presence of the second seed depends on how close they are to each other.

In general, for the two larger systems ($L22$ and $L26$), the probability to grow to macroscopic dimensions depends on the structure of the seeds and not on the volume of the simulation box. (There is a small deviation for systems with the squeezed bcc seeds, which is nevertheless within the error bars.) Also the flux out of the initial state is the same for similar seed structures, such that the frequency of the nucleating events is essentially independent of the system size.

For the smaller system ($L18$), however, the presence of the second seed increases both, the value of the flux through the first interface as well as the probability to proceed to larger cluster sizes after leaving the initial state. Thus, the overall nucleation rate is influenced not only by the structure of the seeds but also by the ability of the seeds to maintain a certain separation between them, which follows from the analysis of the distances between the seeds along transition trajectories presented in the next section. Apparently, there is a certain distance between the seeds, which is adopted in larger systems when the seeds are allowed to move freely. In the smaller system, where this distance roughly corresponds to half of the simulation box edge, seeds are driven closer together ("interacting" through periodic boundary conditions), which increases the probability to include the second seed into the crystalline cluster and hence proceed into the fully crystalline state.

To extract the effect of the relative distance of the seeds, we also studied crystal nucleation in the presence of seeds with fixed relative distances ($D9$, $D11$, and $D13$). The overall system size is comparable to $L26$ for the corresponding freely moving seeds. The obtained nucleation rates are similar only for $D9$ and smaller than those of mobile seeds for $D11$ and $D13$. The values of the flux out of the initial state slightly increase with the decreasing distance between the seeds, but are comparable among themselves as well as with those of the $L26$ system. Deducting the volume effects, we see that the reactive positive flux in Figure 2 coincides with the values obtained in the two larger systems $L22$ and $L26$ for the smallest distance between the seeds ($D9$) and lies below them for $D11$ and $D13$. Here, we refer to the results presented in the next section, which indicate that the average distance between the mobile seeds in $L26$ (and to some extend also in $L22$) is comparable with that in $D9$. Thus, the distance $D = 9$, which we initially selected by chance, and the corresponding reactive flux appear to be intrinsic for the crystal nucleation in the presence of two cubic seeds. We also note that a comparable reactive flux in the presence of fcc seeds separated by a larger distance is an indication that the crystalline clusters formed on one of the seeds grow beyond the critical size when they reach the range of influence of the second seed. For bcc seeds, this flux slightly depends on the distance between the seeds (for clusters larger than a certain size), thus, at the intermediate seed separation, the second seed is close enough to influence the crystalline cluster (formed on one of the seeds) in the vicinity of the free energy barrier. Keeping in mind our previous observation[34] that the critical clusters in the presence of a regular bcc seed are on average considerably larger than in the presence of a regular fcc seed, we conclude that also in the presence of two seeds the critical cluster size varies with the seed structure.

Icosahedral Seeds. The effect of icosahedral seeds on the value of crystal nucleation rate is relatively small in comparison to the impact of cubic seeds. In particular, as can be seen in Figure 3 (exact values are provided in the Supporting Information or can be worked out from Table 2), reactive flux densities at the border of the initial state in the presence of all icosahedral seeds considered correspond to the values of a homogeneous system, actually indicating that the nucleation of small crystallites proceeds homogeneously. Similarly, the flux out of the initial state is not essentially changed by the presence of single icosahedral seeds (Table 3). For single seeds with regular icosahedral structure, one could imagine that the density of the flux out of the initial state decreases with the simulation box volume. Considering that there is a small volume around the seed avoided by crystalline clusters, this is a tendency which one would expect, but the effect is very small.

Nevertheless, the impact of the presence of the seeds becomes noticeable as the reactive flux proceeds to larger crystallites and influences the crystallization rate. Hence, the rate obtained in the presence of icosahedral seeds separated by $D = 9$, which is the smallest rate we have seen in our systems, is approximately five times smaller than the rate measured for $D = 13$. Crystal nucleation rates without seeds and with other icosahedral seeds lie inbetween. Thus, the presence of regular icosahedral seeds with fixed seed-to-seed separation can slightly increase but just as well decrease the crystal nucleation rate compared to homogeneous crystal nucleation, depending on the distance between the seeds. When seeds are allowed to move, the modification of the reaction rates is more modest, yet the values obtained in the presence of icosahedral seeds can again be either larger (regular seeds) or smaller (squeezed seeds) than the homogeneous rates.

A closer look at the evolution of the reactive fluxes with the increasing cluster size presented in Figure 2, reveals that the late stages of crystal nucleation are comparable to the homogeneous systems only in the presence of squeezed icosahedral seeds. Here, the values of the reactive fluxes essentially reproduce those found in the homogeneous systems at matching simulation box volumes. There is a slight (initial)

DOI: 10.1021/acs.jpcb.6b06510
J. Phys. Chem. B 2016, 120, 9230−9239

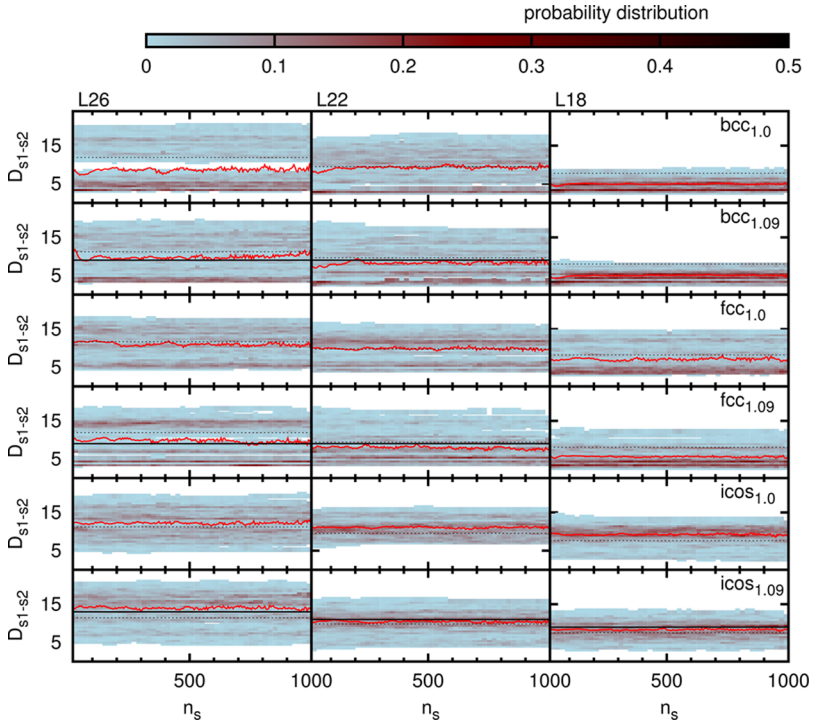

Figure 4. Distribution of the distances between the central particles of the seeds color-coded according to their relative occurrence probability (as a fraction of configurations in which a certain distance is measured) for a given cluster size n_s. Red solid lines indicate the average values in the respective system for a given cluster size, while the black dotted lines denote the average distance between the seeds in the initial state. Black solid lines indicate the distances between the seeds of $D = 9$ for regular cubic seeds in $L26$ and $L22$, and of $D = 13$, $D = 11$, and $D = 9$ for regular icosahedral seeds in $L26$, $L22$, and $L18$, respectively. To improve the statistics, the cluster sizes were sampled in steps of 20, and the distances were sampled in steps of 0.5.

decrease of the positive reactive flux, which finally saturates to the homogeneous plateau. In a previous study,[33] we found that, from time to time, crystals form on a squeezed icosahedral seed, which is also true for the current investigation (results not shown but can be inferred from the Supporting Information). There, we have also seen that the size of the critical clusters formed on the squeezed icosahedral seed is smaller than of those nucleated homogeneously. Thus, we associate the initial decrease of the probability to grow to larger clusters sizes with the possibility of formation of crystalline clusters on the seeds. Aside from that, the reaction rates obtained in the process of homogeneous and crystal nucleation in the presence of squeezed icosahedral seeds are very close to each other.

In contrast, as demonstrated in Figure 2, the freely moving regular seeds in three boxes of different size $L18$, $L22$, and $L26$ almost exactly reproduce the reactive fluxes obtained in the larger box with fixed distances between the seeds, $D9$, $D11$, and $D13$, respectively. The analysis of the transition paths presented in the next section revealed that the average distance between the mobile seeds in these systems is close to the respective fixed distances in the larger system. Apparently, the reaction seen in the presence of regular icosahedral seeds is heterogeneous, but the crystals nucleate far away from the seeds. In addition, what is particularly puzzling is the increase of the crystal nucleation rates with increasing distance between the regular icosahedral seeds. Considering the fact that a single icosahedral seed does not modify the crystal nucleation rate, we have to assume that a further increase of the seed-to-seed separation will result in a reduction of the crystal nucleation rate.

Transition Path Analysis. The presence of pre-structured seeds has an impact not only on the crystal nucleation rates, but also modifies the transition scenario. To study the crystallization mechanism in details, we selected 100 TIS trajectories that reached the crystalline region in TIS simulations and integrated them to crystalline cluster sizes of $n_s \geq 1000$. At these sizes, the structural composition of the crystals becomes similar to those nucleated in a homogeneous system.

We started by analyzing the structural composition of the crystallizing clusters (Supporting Information), which essentially resembles the composition found earlier for the crystallization on single structured seeds.[33,34] Because of the slightly modified definition of crystallinity,[44] however, we found less particles identified as being in a bcc environment. Apparently, the optimized thresholds clarify the picture of the transition following the Ostwald's step rule. Thus, in our case of the undercooled LJ fluid, the formation of the fcc phase stable in bulk is preceded by the formation of the metastable bcc phase, which requires the crossing of a lower free energy barrier and then transforms into the fcc phase. The heterogeneous crystallization on bcc and fcc seeds results in the formation of structures commensurate with the seed structures, but the composition of bulk crystals is recovered as the nucleating clusters grow. The crystalline clusters in the presence of icosahedral seeds have a structure similar to crystals formed by homogeneous crystallization, although there are indications to the rare appearance of icosahedrally structured crystals formed on the seeds with squeezed icosahedral structure, also seen earlier.[33]

Comparatively more informative is the analysis of the relative distances between the mobile seeds along the transition and the separations between the seeds and the crystallizing cluster. The distributions of the distances between the seeds are

DOI: 10.1021/acs.jpcb.6b06510
J. Phys. Chem. B 2016, 120, 9230−9239

summarized in Figure 4 for all types of the seeds, and we refer to the Supporting Information for the results on the distances between the seeds and the crystalline cluster. In the following, we consider cubic seeds and seeds with icosahedral structure separately.

Face- and Body-Centered Cubic Seeds. In general, crystals tend to nucleate on one of the cubic seeds present in the undercooled fluid, as can be inferred from the distribution of the closest separations between the particles of the seeds and of the crystalline cluster, which is presented in the Supporting Information. In nearly all configurations along crystallizing paths, we find that the crystalline clusters are in close contact with one of the seeds. There are a few exceptions for small clusters, but the distance between the crystal and the seed we see in these cases is relatively small. In contrast, the probability of the inclusion of the second seed into the crystal is not definite and depends not only on the size of the system but also on the structure of the seeds. Thus, both squeezed bcc seeds in the smallest system ($L18$) belong to the crystal, if the size of the crystal is large enough. For smaller crystals and other types of seeds in this system, it is the most probable configuration. In the larger systems ($L22$ and $L26$), the probability to find the second seed outside of the small crystalline clusters is larger, but the mean distance between the clusters and these seeds decreases as the crystals grow and the fraction of configurations in which the second seed is included into them increases.

These findings confirm our hypothesis that crystal nucleation in the presence of two structured seeds is only indirectly influenced by the presence of the second seed, which is included into the crystallizing cluster only if, due to the size of the system, the initial separation between the seeds is relatively small.

The last observation raises the question whether there is a typical separation assumed by the seeds in the course of the transition, at which the crystallizing cluster formed on one of the seeds is influenced by the second seed. As demonstrated in Figure 4, we again have to differentiate between the smallest $L18$ and the two larger systems $L22$ and $L26$. In the larger systems, one finds configurations with all possible distances between the seeds. The average separation, however, is comparable for a given seed structure, which explains why similar reactive fluxes occur in these systems. For regular seeds, Figure 4 also indicates the separation of $D = 9$, which in the systems with a fixed relative distance resulted in a reactive flux that is comparable to the flux found in larger systems with mobile seeds. Apparently, the average distance fluctuates very close to this value in both $L22$ and $L26$ systems. In the smaller system and particularly in the presence of bcc structures, on the other hand, the seeds are closer to each other and the reactive flux is increased.

Furthermore, Figure 4 also provides the average values of the seed-to-seed separations found in the initial fluid state (corresponding distributions can be found in the Supporting Information). For all but one system ($L22$ with squeezed bcc seeds, where they are equal) the mean distances between the seeds in the transition paths are smaller than the corresponding distances in the initial state, which indicates that a certain fraction of the initial flux out of the initial state, with seed separations below average, will be better suited for the transition than the other.

Icosahedral Seeds. The mechanism of the crystallization transition in the presence of icosahedral seeds is very different from that in the presence of cubic seeds. The crystals nucleate mainly in the bulk, although there are some configurations along the transition paths in which the seed particles are in the neighborhood of the cluster. (The optimized scheme used here to find particles in the crystalline environment does not recognize the particles of icosahedral seeds as solid.) For squeezed seeds, there are also some trajectories, along which the crystals form around one of the icosahedral seeds. On average, however, the distance between the crystalline cluster and the icosahedral seeds is rather large, although it decreases as the cluster grows. Thus, at this stage of crystal nucleation, we do not see any indication that a growing crystalline cluster expels an incommensurate seed as seen in colloidal composite materials,[48] where foreign particles accumulated on the grain boundaries of growing crystals. On the contrary, in the presence of icosahedral seeds, we see that the average distance between the seeds fluctuates around a value which increases with the simulation box size. Thus, we cannot confirm that the incommensurate seeds (if seen as foreign particles) tend to cluster together. The average seed-to-seed distances during the transition lie distinctly above the mean values of the initial state, indicating that, in comparison to cubic seeds, a different fraction of the initial reactive flux is important for a successful transition in the presence of icosahedral seeds. Moreover, for regular structures, the distance between the moving seeds is close to $D = 9$ (in $L18$), $D = 11$ (in $L22$), and $D = 13$ (in $L26$), which we used as fixed distances between the regular icosahedral seeds ($D9$, $D11$, and $D13$). As we stated in the previous section, these findings explain the equality of the respective reactive fluxes, indicating that their value is determined only by the distance between the seeds.

CONCLUSIONS

Pairs of tiny structured seeds influence the process of crystal nucleation in an undercooled LJ fluid in essentially two ways. First, they may serve as nucleation sites for heterogeneous crystallization, if their structure is (at least partly) commensurate with the bulk crystalline structure. Second, they influence the probability of the crystalline clusters to grow to macroscopic dimensions. The effects that the presence of seeds has on the crystallization largely depend on the structure of the seeds and on the distance between the seeds.

In the early nucleation stages, bcc and fcc seeds enhance the formation of the crystalline clusters, for which the seeds act as nucleation sites for heterogeneous crystallization. In the two larger systems considered, the positive reactive flux out of the initial state is independent of the volume of the simulation box, which is a sign of heterogeneous nucleation. In the smaller system, where the seeds are closer to each other, this initial flux is slightly increased. We recover the expected linear dependence of the reactive flux on the number of nucleation sites only partially, since in the presence of single seeds in the larger systems both homogeneous and heterogeneous crystal nucleation contribute to the flux out of the initial state. We also found that the presence of single squeezed seeds with cubic structure may effectively suppress the initial flux density relative to the homogeneous case. The effect is relatively small and vanishes as the transition proceeds, since the probability of the pathways contributing to the fraction of the flux associated with heterogeneous crystal nucleation to evolve to the fully crystalline states is higher than the corresponding probability of the pathways in which crystals formed homogeneously. The presence of icosahedral seeds, on the other hand, does not change the reactive flux out of the initial state, as already seen

DOI: 10.1021/acs.jpcb.6b06510
J. Phys. Chem. B 2016, 120, 9230−9239

for single icosahedral seeds, and one recovers the flux values of homogeneous crystal nucleation also in the presence of two seeds. If these icosahedral seeds have a regular lattice spacing, crystalline clusters do not form on these seeds but the avoided volume is relatively small such that the value of the flux is not substantially altered by this fact. In the presence of slightly squeezed icosahedral seeds, the crystals nucleate also mainly in the bulk, but there is a finite probability that the crystal forms near one of the seeds.

As small nucleated crystallites evolve to larger sizes, the presence of the second seed modifies the probability of these cluster to grow to macroscopic dimensions. Hence, crystal nucleation rates are determined by the impact of the second seed for all but the slightly squeezed icosahedral seeds. We found that the effect depends on the distance between the seeds. Both bcc and fcc seeds, if allowed to move and provided enough space, assume a certain distance between them, which results in a similar evolution of the reactive flux. If a smaller or larger distance is imposed on the separation between the seeds, the flux is either increased or decreased, respectively. For regular icosahedral seeds, the average seed-to-seed separation of freely moving seeds along the transition pathways increases with the system size. Contrary to the case of cubic seeds, the increase of the fixed distance between regular icosahedral seeds results in an increase of the crystal nucleation rate.

In summary, nucleation rates computed here for systems containing seeds of different structures indicate that the classical picture of foreign particles simply offering sites for heterogeneous nucleation applies only in the low density limit. As soon as the seeds are close enough to each other, they influence not only the initial nucleation probability but also the probability of the evolution of the crystallite to macroscopic dimensions. Even in the presence of regular icosahedral seeds, which do not trigger heterogeneous nucleation, the nucleation rate is nevertheless affected by the seeds. In contrast to the case of cubic seeds, however, we could not localize a special seed-to-seed separation which is assumed by the seeds in the course of the transition. Moreover, the nucleation rate associated with the largest distance between the seeds lies above the homogeneous rate. Thus, a further increase of the distance between the seeds should eventually lead to a turnover and subsequent decrease of the crystal nucleation rate, since the presence of a single seed does not modify the homogeneous crystal nucleation rate.

■ ASSOCIATED CONTENT

Supporting Information

The Supporting Information is available free of charge on the ACS Publications website at DOI: 10.1021/acs.jpcb.6b06510.

Distributions of the distances between the seeds in the initial state; densities of the positive reactive flux out of the initial state; distributions of distances between crystalline clusters and the seeds; structural compositions of crystallizing clusters (PDF)

■ AUTHOR INFORMATION

Corresponding Author

*E-mail: swetlana.jungblut@univie.ac.at Phone: +43 (0)1 4277-51262. Fax: +43 (0)1 4277-851262.

Notes

The authors declare no competing financial interest.

■ ACKNOWLEDGMENTS

The computational results presented have been achieved using the Vienna Scientific Cluster (VSC). We acknowledge financial support of the Austrian Science Fund (FWF) within the Project V 305-N27 as well as SFB ViCoM (Grant F41).

■ REFERENCES

(1) Kelton, K. F.; Greer, A. L. *Nucleation in Condensed Matter*; Elsevier: Amsterdam, 2010.
(2) Gasser, U. Crystallization in three- and two-dimensional colloidal suspensions. *J. Phys.: Condens. Matter* **2009**, *21*, 203101.
(3) Herlach, D. M.; Klassen, I.; Wette, P.; Holland-Moritz, D. Colloids as model systems for metals and alloys: a case study of crystallization. *J. Phys.: Condens. Matter* **2010**, *22*, 153101.
(4) Sear, R. P. The non-classical nucleation of crystals: microscopic mechanisms and applications to molecular crystals, ice and calcium carbonate. *Int. Mater. Rev.* **2012**, *57*, 328−356.
(5) Palberg, T. Crystallization kinetics of colloidal model suspensions: recent achievements and new perspectives. *J. Phys.: Condens. Matter* **2014**, *26*, 333101.
(6) Niedermeier, D.; Hartmann, S.; Shaw, R. A.; Covert, D.; Mentel, T. F.; Schneider, J.; Poulain, L.; Reitz, P.; Spindler, C.; Clauss, T.; et al. Heterogeneous freezing of droplets with immersed mineral dust particles − measurements and parameterization. *Atmos. Chem. Phys.* **2010**, *10*, 3601−3614.
(7) de Villeneuve, V. W. A.; Verboekend, D.; Dullens, R. P. A.; Aarts, D. G. A. L.; Kegel, W. K.; Lekkerkerker, H. N. W. Hard sphere crystal nucleation and growth near large spherical impurities. *J. Phys.: Condens. Matter* **2005**, *17*, S3371−S3378.
(8) Cacciuto, A.; Auer, S.; Frenkel, D. Onset of heterogeneous crystal nucleation in colloidal suspensions. *Nature* **2004**, *428*, 404−406.
(9) de Villeneuve, V. W. A.; Dullens, R. P. A.; Aarts, D. G. A. L.; Groeneveld, E.; Scherff, J. H.; Kegel, W. K.; Lekkerkerker, H. N. W. Colloidal hard-sphere crystal growth frustrated by large spherical impurities. *Science* **2005**, *309*, 1231−1233.
(10) Allahyarov, E.; Sandomirski, K.; Egelhaaf, S. U.; Löwen, H. Crystallization seeds favour crystallization only during initial growth. *Nat. Commun.* **2015**, *6*, 7110.
(11) Dijkstra, M. Capillary Freezing or Complete Wetting of Hard Spheres in a Planar Hard Slit? *Phys. Rev. Lett.* **2004**, *93*, 108303.
(12) Page, A. J.; Sear, R. P. Freezing in the bulk controlled by prefreezing at a surface. *Phys. Rev. E* **2009**, *80*, 031605.
(13) Hedges, L. O.; Whitelam, S. Patterning a surface so as to speed nucleation from solution. *Soft Matter* **2012**, *8*, 8624−8635.
(14) Sandomirski, K.; Walta, S.; Dubbert, J.; Allahyarov, E.; Schofield, A. B.; Löwen, H.; Richtering, W.; Egelhaaf, S. U. Heterogeneous crystallization of hard and soft spheres near flat and curved walls. *Eur. Phys. J.: Spec. Top.* **2014**, *223*, 439−454.
(15) Heni, M.; Löwen, H. Surface Freezing on Patterned Substrates. *Phys. Rev. Lett.* **2000**, *85*, 3668−3671.
(16) Heni, M.; Löwen, H. Precrystallization of fluids induced by patterned substrates. *J. Phys.: Condens. Matter* **2001**, *13*, 4675−4696.
(17) Cacciuto, A.; Frenkel, D. Simulation of colloidal crystallization on finite structured templates. *Phys. Rev. E* **2005**, *72*, 041604.
(18) Dziomkina, N. V.; Vancso, G. J. Colloidal crystal assembly on topologically patterned templates. *Soft Matter* **2005**, *1*, 265−279.
(19) Xu, W.-S.; Sun, Z.-Y.; An, L.-J. Heterogeneous crystallization of hard spheres on patterned substrates. *J. Chem. Phys.* **2010**, *132*, 144506.
(20) Xu, W.-S.; Sun, Z.-Y.; An, L.-J. Assembly of body-centered cubic crystals in hard spheres. *Eur. Phys. J. E: Soft Matter Biol. Phys.* **2011**, *34*, 47.
(21) Tóth, G. I.; Tegze, G.; Pusztai, T.; Gránásy, L. Heterogeneous Crystal Nucleation: The Effect of Lattice Mismatch. *Phys. Rev. Lett.* **2012**, *108*, 025502.
(22) Dorosz, S.; Schilling, T. On the influence of a patterned substrate on crystallization in suspensions of hard spheres. *J. Chem. Phys.* **2012**, *136*, 044702.

DOI: 10.1021/acs.jpcb.6b06510
J. Phys. Chem. B 2016, 120, 9230−9239

(23) Zhang, H.; Peng, S.; Mao, L.; Zhou, X.; Liang, J.; Wan, C.; Zheng, J.; Ju, X. Freezing of Lennard-Jones fluid on a patterned substrate. *Phys. Rev. E* **2014**, *89*, 062410.
(24) Mithen, J. P.; Sear, R. P. Epitaxial nucleation of a crystal on a crystalline surface. *EPL* **2014**, *105*, 18004.
(25) Mithen, J. P.; Sear, R. P. Computer simulation of epitaxial nucleation of a crystal on a crystalline surface. *J. Chem. Phys.* **2014**, *140*, 084504.
(26) Lederer, A.; Franke, M.; Schöpe, H. J. Heterogeneous nucleation and microstructure formation in colloidal model systems with various interactions. *Eur. Phys. J.: Spec. Top.* **2014**, *223*, 389−407.
(27) Hermes, M.; Vermolen, E. C. M.; Leunissen, M. E.; Vossen, D. L. J.; van Oostrum, P. D. J.; Dijkstra, M.; van Blaaderen, A. Nucleation of colloidal crystals on configurable seed structures. *Soft Matter* **2011**, *7*, 4623−4628.
(28) Schöpe, H. J.; Wette, P. Seed- and wall-induced heterogeneous nucleation in charged colloidal model systems under microgravity. *Phys. Rev. E* **2011**, *83*, 051405.
(29) Wang, H.; Gould, H.; Klein, W. Homogeneous and heterogeneous nucleation of Lennard-Jones liquids. *Phys. Rev. E* **2007**, *76*, 031604.
(30) Browning, A. R.; Doherty, M. F.; Fredrickson, G. H. Nucleation and polymorph selection in a model colloidal fluid. *Phys. Rev. E* **2008**, *77*, 041604.
(31) van Teeffelen, S.; Likos, C. N.; Löwen, H. Colloidal Crystal Growth at Externally Imposed Nucleation Clusters. *Phys. Rev. Lett.* **2008**, *100*, 108302.
(32) Neuhaus, T.; Schmiedeberg, M.; Löwen, H. Crystallization induced by multiple seeds: Dynamical density functional approach. *Phys. Rev. E* **2013**, *88*, 062316.
(33) Jungblut, S.; Dellago, C. Heterogeneous crystallization on tiny clusters. *EPL* **2011**, *96*, 56006.
(34) Jungblut, S.; Dellago, C. Crystallization on prestructured clusters. *Phys. Rev. E* **2013**, *87*, 012305.
(35) Jungblut, S.; Dellago, C. On the reaction coordinate for seeded crystallisation. *Mol. Phys.* **2015**, *113*, 2735−2741.
(36) Andersen, H. C. Molecular dynamics simulations at constant pressure and/or temperature. *J. Chem. Phys.* **1980**, *72*, 2384−2393.
(37) Kamberaj, H.; Low, R. J.; Neal, M. P. Time reversible and symplectic integrators for molecular dynamics simulations of rigid molecules. *J. Chem. Phys.* **2005**, *122*, 224114.
(38) Berendsen, H. J. C.; Postma, J. P. M.; van Gunsteren, W. F.; DiNola, A.; Haak, J. R. Molecular dynamics with coupling to an external bath. *J. Chem. Phys.* **1984**, *81*, 3684−3690.
(39) van Erp, T. S.; Moroni, D.; Bolhuis, P. G. A novel path sampling method for the calculation of rate constants. *J. Chem. Phys.* **2003**, *118*, 7762−7774.
(40) van Erp, T. S.; Bolhuis, P. G. Elaborating transition interface sampling methods. *J. Comput. Phys.* **2005**, *205*, 157−181.
(41) Moroni, D.; ten Wolde, P. R.; Bolhuis, P. G. Interplay between Structure and Size in a Critical Crystal Nucleus. *Phys. Rev. Lett.* **2005**, *94*, 235703.
(42) Steinhardt, P. J.; Nelson, D. R.; Ronchetti, M. Bond-orientational order in liquids and glasses. *Phys. Rev. B: Condens. Matter Mater. Phys.* **1983**, *28*, 784−805.
(43) ten Wolde, P. R.; Ruiz-Montero, M. J.; Frenkel, D. Numerical calculation of the rate of crystal nucleation in a Lennard-Jones system at moderate undercooling. *J. Chem. Phys.* **1996**, *104*, 9932−9947.
(44) Jungblut, S.; Singraber, A.; Dellago, C. Optimising reaction coordinates for crystallisation by tuning the crystallinity definition. *Mol. Phys.* **2013**, *111*, 3527−3533.
(45) Ostwald, W. Studien über die Bildung und Umwandlung fester Körper. *Z. Phys. Chem.* **1897**, *22*, 289−315.
(46) Stranski, I. N.; Totomanow, D. Keimbildungsgeschwindigkeit und Ostwaldsche Stufenregel. *Z. Phys. Chem.* **1933**, *A163*, 399−408.
(47) ten Wolde, P. R.; Frenkel, D. Homogeneous nucleation and the Ostwald step rule. *Phys. Chem. Chem. Phys.* **1999**, *1*, 2191−2196.
(48) Ghofraniha, N.; Tamborini, E.; Oberdisse, J.; Cipelletti, L.; Ramos, L. Grain refinement and partitioning of impurities in the grain boundaries of a colloidal polycrystal. *Soft Matter* **2012**, *8*, 6214−6219.

DOI: 10.1021/acs.jpcb.6b06510
J. Phys. Chem. B 2016, 120, 9230−9239